

Electronic Supporting Information

Highly efficient recovery of high-purity Cu, PVC, and phthalate plasticizer from waste wire harnesses through PVC swelling and rod milling

Harendra Kumar, Shogo Kumagai, Tomohito Kameda, Yuko Saito, Toshiaki Yoshioka*

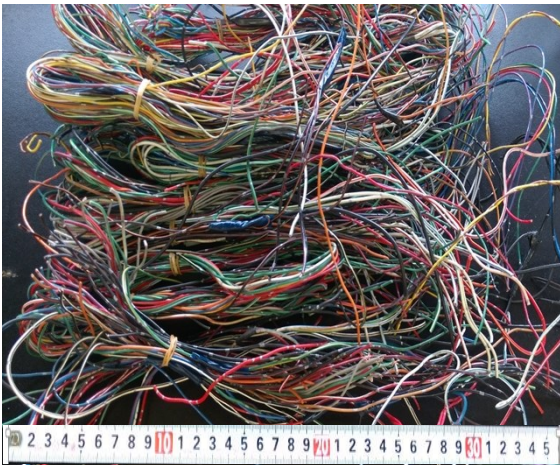
Graduate School of Environmental Studies, Tohoku University, 6-6-07 Aoba Aramaki-Aza, Aoba-ku, Sendai, Miyagi 980-8579, Japan

***Corresponding author.** Email: kumagai@tohoku.ac.jp, tel./fax: +81-22-795-7212

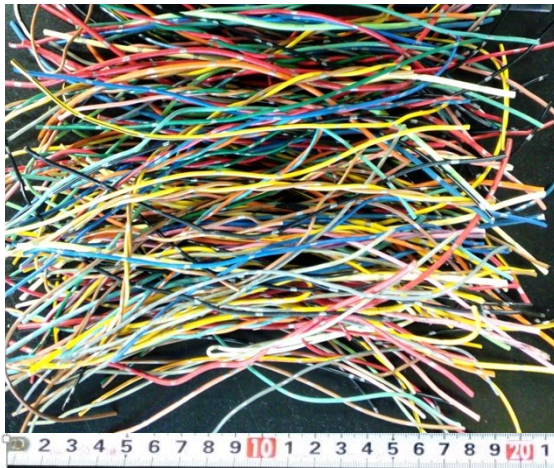
Supplementary 1: Waste wire harness assembly and size distribution of collected cables



(a)



(b)



(c)



(d)

Fig. S1-1. Images of (a) as-received waste wire harnesses, (b) sorted cables, (c) cables cut into 20-cm-long pieces, and (d) distribution of cables in wire harness assembly.

The wire harness assembly consisted cables with diameters of 1.0 (samples 1 and 2), 1.2 (samples 3–9), and 2.0 mm (sample 10), which accounted for 15, 70, and 15% of the total weight, respectively. Table S1 presents the elemental compositions (wt%) of the collected cables (samples 1–10 in Fig. S1-1(d)).

Table S1-1. Elemental compositions of collected cables

Cable diameter [mm]	Weight composition [wt%]				
	C	H	N	Cl	Balance ^a
1.0	46.7	6.2	– ^b	35.7	11.5
1.2	45.4	5.9	–	35.3	13.4
2.0	45.0	5.8	–	33.4	15.8

^aMainly oxygen and ash. ^bNot detected.

Supplementary 2: Quantitation of DINP in harness samples via dissolution/precipitation method and subsequent ¹H NMR spectroscopy using fumaric acid as internal standard

During the dissolution/precipitation process, the waste cables were magnetically stirred for 2 h at 21 °C in a glass bottle filled with tetrahydrofuran (100 mL). After the complete dissolution of the PVC coatings, the Cu wires were collected and weighed. The insoluble PVC constituents were separated by the centrifugation (H-19F, Kokusan Co., Ltd., Japan) of the solution at 3000 rpm for 20 min. The supernatant was mixed with ethanol (100 mL) and sonicated for 2 h to achieve complete PVC precipitation. The precipitated PVC was separated by centrifugation as described above and dried in a vacuum oven at 60 °C, while the collected solution was distilled using a water bath (50 °C) equipped with a condenser (operated at –5 to –10 °C) to recover the plasticizer and regenerate the solvent. As the recovered plasticizer contained traces of PVC, more ethanol (50 mL) was added to it for purification. The PVC particles were separated by centrifugation, and the recovered solvent was collected in a fresh flask for further distillation. The regenerated PVC, solvent, and plasticizer were finally collected, and their amounts were measured. A schematic of the process flow is shown in Fig. S2-1.

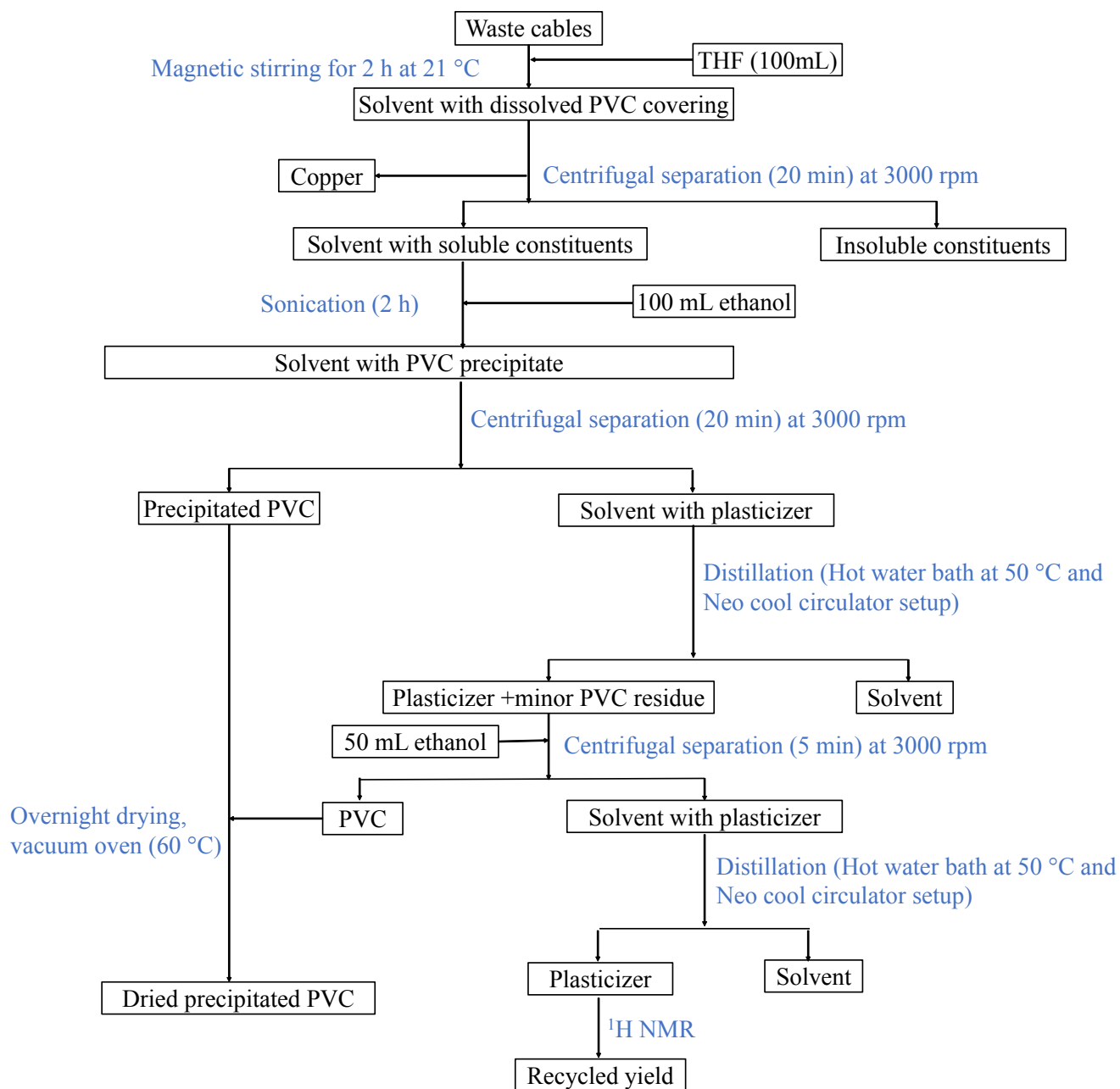


Fig. S2-1. Flow chart for recovery of plasticizer from cables.

Fig. S2-2 shows the chemical structure of DINP while Fig S2-3 (a) shows the ^1H NMR spectrum of pristine DINP and (b) shows that of the pristine DINP superimposed onto DINP extracted via dissolution/precipitation

from the cables. It is clear that the plasticizer in the cables was indeed DINP. The peaks in the ^1H NMR spectrum of DINP are listed in Table S2-1.

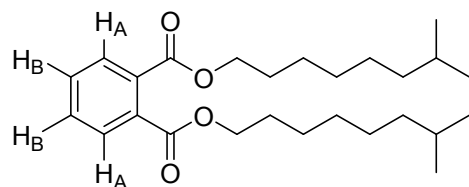
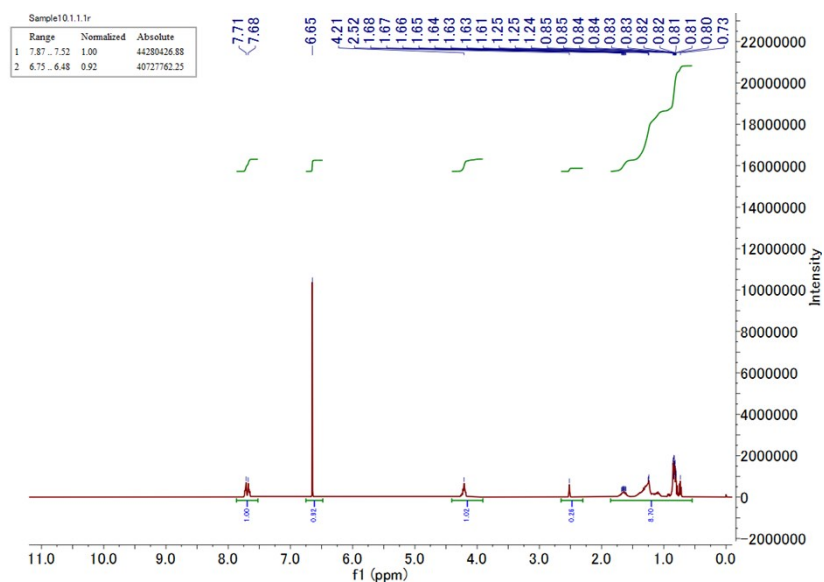
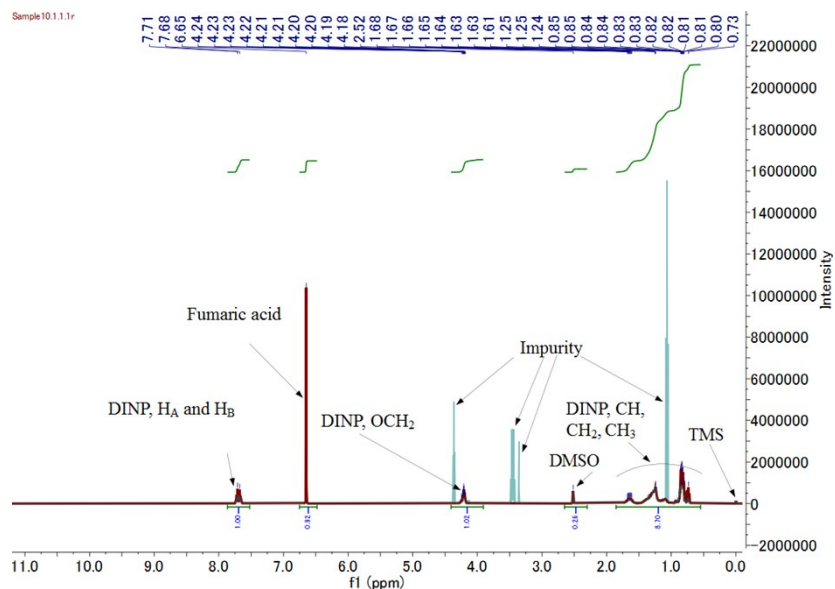


Fig. S2-2 Chemical structure of DINP.



(a)



(b)

Fig S2-3 ^1H NMR spectrum of (a) pure DINP with fumaric acid and (b) pure DINP spectrum (red lines) superimposed onto extracted DINP by dissolution/precipitation (blue lines) from cable samples. Impurity belongs to tetrahydrofuran (THF)/ethanol.

Table S2-1. Peaks in ^1H NMR spectrum of DINP

δ (ppm)	Assignment	Coupling constant (J)
7.71	H_A	2H, H_1 , dd, $^3J_{\text{A-B}} = 5.6$ Hz, $^4J_{\text{A-B}} = 3.2$ Hz
7.68	H_B	2H, H_2 , dd, $^3J_{\text{B-A}} = 5.6$ Hz, $^4J_{\text{B-A}} = 3.2$ Hz
4.20–4.21	OCH_2	(~4H, m)
1.68–0.73	CH, CH_2 , CH_3	(~34H, m).
6.65	Standard peak (fumaric acid)	
2.51–2.52	Solvent peak (DMSO)	

The regenerated solvent (*n*-butyl acetate) was absolutely pure, as shown in Fig. S2-4, which provides its ^1H NMR spectrum. However, after distillation, the recovered plasticizer contained a trace amount of *n*-butyl acetate as an impurity, as shown in Fig. S2-5, in which the spectrum of pure DINP is superimposed onto that of the DINP extracted from the cables. Thus, fumaric acid was used to estimate the amount of DINP present in the cables. To calculate the value of coefficient K for DINP, a fumaric acid (m_F)/DINP (m_DINP) mixture of known composition was dissolved in dimethyl sulfoxide and analyzed using ^1H NMR spectroscopy. The area under the fumaric acid peak at 6.65 ppm (S_F) and that under the DINP peaks at 7.68 and 7.71 ppm (S_DINP) were determined (Fig. S3-2 and Table S3-1) and used to calculate K as follows:

$$K = m_\text{DINP} \times S_\text{F} \times M_\text{F} / (M_\text{DINP} \times S_\text{DINP} \times m_\text{F}), \quad (\text{S1})$$

where K [–] is the coefficient to be calculated; M_DINP [g/mol] is the molecular weight of DINP; m_DINP [mg] is the weight of DINP added; S_DINP [–] is the area under the peaks at 7.68 and 7.71 ppm, which are related to the coupling of the *ortho*- (H_A and H_B) DINP protons; M_F [g/mol] is the molecular weight of fumaric acid; m_F [mg] is the weight of fumaric acid added; and S_F [–] is the area under the fumaric acid peak at 6.65 ppm.

To calculate the recycling yield (Y_{recy}) of DINP in a 12.8-g waste cable sample, we first calculated the weight of pure DINP (W_{DINP}) in the NMR sample (which contained a known amount of the extracted DINP (W_{ext}) and a known amount of fumaric acid (m_{F})) using Eq. S2. Then, we used the purity factor (W_{DINP} divided by W_{ext}) to calculate the weight of the pure recovered DINP (W_{recy}) in the total DINP ($W_{\text{ext total}}$) extracted via dissolution/precipitation from the 12.8-g waste cable sample as follows:

$$W_{\text{DINP}} = M_{\text{DINP}} \times S_{\text{DINP}} \times m_{\text{F}} \times K / (S_{\text{F}} \times M_{\text{F}}), \quad (\text{S2})$$

$$W_{\text{recy}} = W_{\text{DINP}} \times W_{\text{ext total}} / W_{\text{ext}}. \quad (\text{S3})$$

This experiment was repeated five times (weight of cable sample = 12.8 g in each case), and the average value of W_{recy} was determined. Then, this value together with the amount of DINP in a 12.8-g cable sample ($W_{\text{DINP in PVC}}$) was used to determine the recycling yield [%] of DINP (Y_{recy}) as follows:

$$Y_{\text{recy}} = 100\% \times W_{\text{recy}} / W_{\text{DINP in PVC}}. \quad (\text{S4})$$

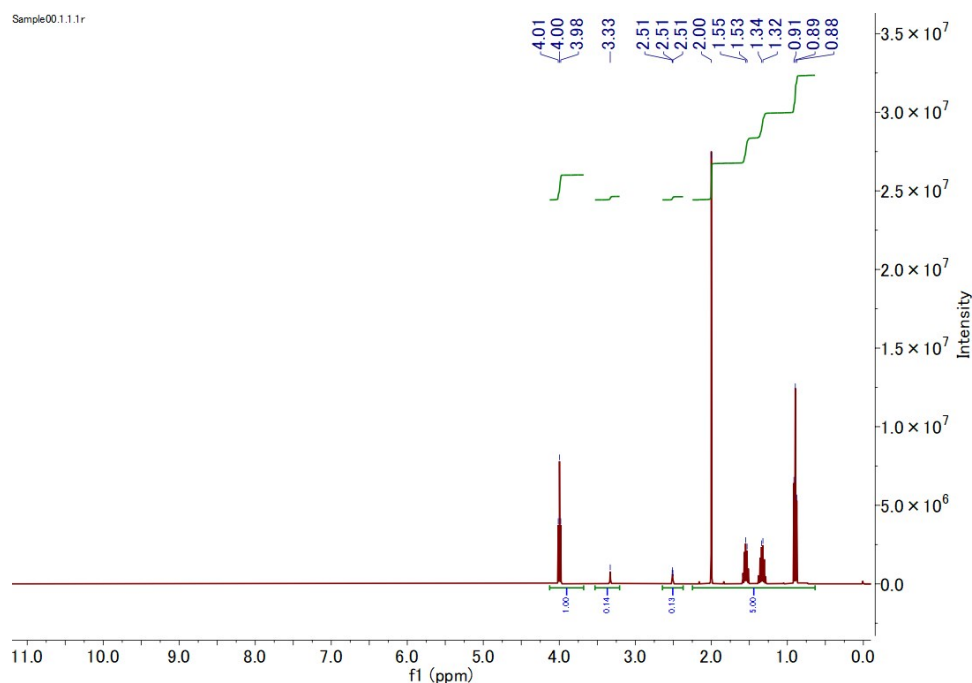


Fig S2-4 ^1H NMR spectrum of recovered solvent (*n*-butyl acetate).

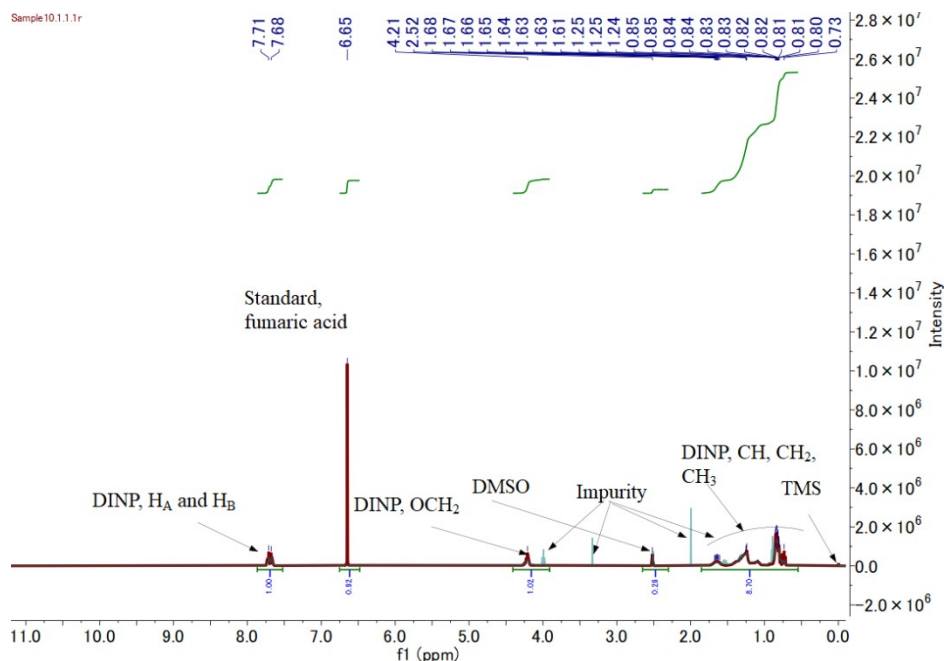


Fig. S2-5 ¹H NMR spectrum of pure DINP (red line, Fig. S2-3 (a)) superimposed onto that of DINP recycled from *n*-butyl acetate collected after extraction for 80 min (blue line). Impurity peaks belong to *n*-butyl acetate.

Supplementary 3: Recovery of Cu and PVC by jigging separation method after milling

Water-jigging-based separation was performed using a jigging separator (Fig. S3-1) fabricated in the laboratory specifically for handling long milled Cu and PVC pieces. However, jigging has been employing for decades for mineral separation. The separation results reported here confirmed that the water jigging method is suitable separating the Cu and PVC pieces after milling. The mixture of Cu wires and swollen PVC coatings was placed on top of the jig screen (425 μm). Then, flowing water caused the swollen PVC pieces to overflow and separate from the Cu wires. For a steady flow of water, the difference in the accelerations¹ of the particles during falling can be determined as follows:

$$dv_p/dt = (1 - \rho_w/\rho_p)g, \quad (S5)$$

where, g , ρ_w , and ρ_p are the acceleration due to gravity, specific gravity of water, and specific gravity of the particles (Cu and PVC), respectively. The drag force was neglected since the particle velocity was low. The duration of the jigg cycle was set to 30 s, as it allowed for the fastest separation, and the process was performed at ~ 25 °C. The large difference in the specific gravities of the Cu wires (8.4 ± 0.5 g/cm³) and the swollen PVC coatings (0.9 ± 0.1 g/cm³) as well as their long sizes allowed for easy separation. Further, because of this large difference, the almost-swollen PVC coatings could also be separated during the first jig cycle.

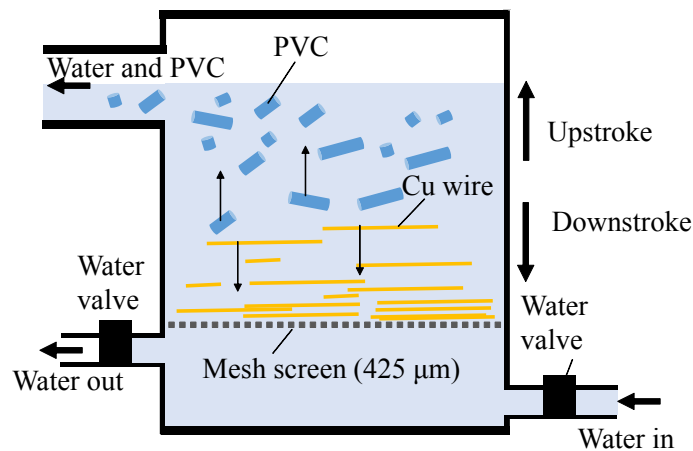


Fig. S3-1. Laboratory-designed apparatus for water jigg separation used in this study.

Supplementary 4: Suggested behaviors of rods and cables during rod milling process

Fig.S4-1 shows the suggested behavior of the rods during the rod milling process (Fig.S4-1(a)) and compares it with that of the balls during ball milling (Fig.S4-1(b)). From the results of the milling tests, it was clear that the crushing of the swollen cables occurs more quickly during rod milling than during ball milling. The separation rate (R_{sep}) of the Cu wires and the PVC coatings during ball milling was slightly improved at a rotating speed of 20 rpm, whereas in the case of rod milling, there was tremendous improvement in R_{sep} at 15 rpm. Thus, it is likely that the rods come in contact with a larger area of the cables bed during each strike,

whereas, in the case of ball milling, some of the balls hit the reactor wall. On the other hand, reducing the rotating speed during ball milling also reduced R_{sep} owing to the decrease in the amount of energy delivered by the balls. In addition, we employed 20-cm-long cables for the milling tests. Thus, it is likely that this reduced the probability of the balls hitting the cables: the higher the number of pieces within the reactor, the greater the probability will be of hitting them. Thus, these behaviors may be specific to the conditions of this study alone.

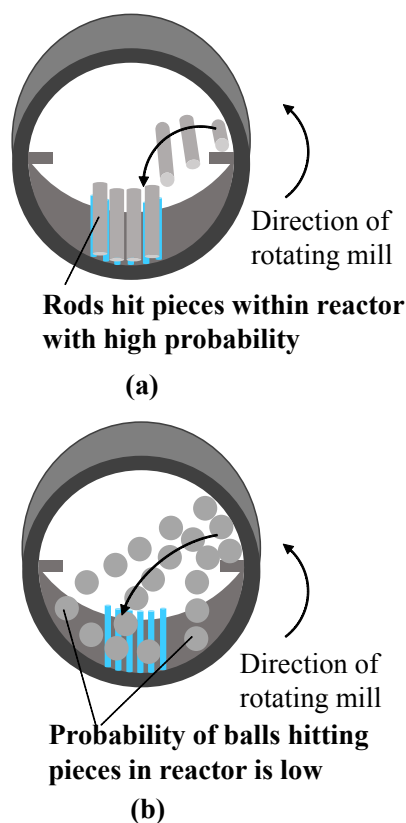


Fig. S4-1: Suggested behaviors of rods and cables during (a) rod milling and (b) conventional ball milling.

References

1. C. K. Gupta, *Chemical Metallurgy: Principles and Practice*, John Wiley & Sons, 2006.